bolic excitons associated with Λ. Whether the exciton effect is also important in the other transitions remains to be investigated.

To help us make sure that our assignment of reflectivity peaks is correct, measurements on samples under uniaxial stress should be performed. That a stress can be exerted on the sample without much complication is another advantage of the wavelength-modulation scheme. The pressure dependence of the reflectivity spectrum should also yield valuable information about hyperbolic excitons associated at various symmetry points.[31]

ACKNOWLEDGMENTS

We would like to thank M. L. Cohen, J. P. Walter, R. Cahn, and C. Y. Fong for many helpful discussions, and M. P. Klein for technical help. This work was done under the asupices of the U. S. Atomic Energy Commission.

[31] E. O. Kane, Phys. Rev. **178**, 1368 (1969).

PHYSICAL REVIEW B VOLUME 1, NUMBER 6 15 MARCH 1970

Infrared Cyclotron Resonance and Related Experiments in the Conduction Band of InSb†

E. J. JOHNSON AND D. H. DICKEY
Lincoln Laboratory, Massachusetts Institute of Technology, Lexington, Massachusetts 02173
(Received 29 August 1969)

We present a comprehensive study of the conduction band of InSb. Experimental observations of fundamental cyclotron-resonance transitions involving the lowest Landau levels and both spin states are reported over a range of magnetic fields from 5 to 35 kG. Additional transitions involving impurities, phonons, cyclotron-resonance harmonics, and spin flip are also observed. The fundamental cyclotron resonance and the spin-flip cyclotron resonance, together with the spin-resonance results of Isaacson, are analyzed in terms of a nonparabolic band theory involving interactions with the six valence bands and allowing the possibility of interactions with more remote bands. A good fit to the nonparabolic band theory is obtained when one is careful to remove effects due to impurities and the electron-phonon interaction. A band-edge effective mass of $0.0139m$ and a band-edge g factor of -51.3 are obtained. An analysis using these values shows that remote band interactions contribute to the value of either the mass or g factor or both by an amount on the order of 10%. The transition energies for cyclotron-resonance harmonics, spin-flip transitions, phonon-assisted cyclotron resonance, and spin resonance as a function of Fermi level have been calculated and give a good fit to the data. This confirms the identification of these transitions and shows that the nonparabolic theory gives the magnetic energy levels correctly to energies as high as 60 meV. A value of 24.4 meV is found for the LO phonon energy. The existence of the phonon-assisted cyclotron resonance is explained on the basis of the mixing of Landau levels by the electron-phonon interaction. The strength of the cyclotron-resonance harmonics is not satisfactorily explained, although several possible mechanisms are proposed. An $H=0$ electron-energy dispersion relation and other related band properties are deduced from the magnetic field results and compared with other experiments.

I. INTRODUCTION

FOR some time there has been a great need for the determination of the precise location of the conduction-band energy levels in InSb, both with and without a magnetic field. Experiments involving excitons,[1] polarons,[2–4] interband absorption,[5] and Raman scattering[6] have been performed. The analysis of these experiments depends critically upon the precise location of the conduction-band energy levels.

We report here a comprehensive study of the conduction band of InSb using infrared cyclotron resonance. We have employed improved techniques to obtain sharp lines with well-resolved structure. Our fit of nonparabolic theory to the experimental results takes into account band interaction effects and provides a precise determination of the band-edge effective mass and effective spin g factor. We identify transitions involving cyclotron-resonance harmonics and transitions involving an LO phonon. From these results, we obtain a measure of the zone center LO phonon energy. A better understanding of the fine structure is

† Work sponsored by the Department of the Air Force.
[1] E. J. Johnson, Phys. Rev. Letters **19**, 352 (1967).
[2] E. J. Johnson and D. M. Larsen, Phys. Rev. Letters **16**, 655 (1966); also D. M. Larsen and E. J. Johnson, in Proceedings of the International Conference on Physics of Semiconductors, Kyoto, 1966, p. 443 (unpublished).
[3] D. H. Dickey, E. J. Johnson, and D. M. Larsen, Phys. Rev. Letters **18**, 599 (1967); see also C. J. Summers *et al.*, Phys. Rev. **170**, 755 (1968).
[4] D. H. Dickey and D. M. Larsen, Phys. Rev. Letters **20**, 65 (1968).
[5] C. R. Pidgeon and R. N. Brown, Phys. Rev. **146**, 575 (1966).
[6] R. E. Slusher, C. K. N. Patel, and P. A. Fleury, Phys. Rev. Letters **18**, 77 (1967).

obtained and the relationship between the various types of transitions is well demonstrated. Additional information is obtained from an analysis of the spin-resonance results of Isaacson.[7]

Cyclotron resonance is well known as a technique for measuring the effective mass of electrons in solids. Most electron energy bands are not simple, however, and cannot be described by a single effective mass independent of energy. Furthermore, interactions, such as those due to electron-phonon effects and to impurities, add complications to the simple band picture. These effects shift the energy levels and add additional absorption lines. In materials where the energy-level separations are sufficiently sensitive to a magnetic field, infrared cyclotron resonance offers considerable advantage over microwave techniques. In the infrared region of the spectrum, it is convenient to vary photon energy continuously over a wide range and obtain energy-level separation as a function of magnetic field. The data thus obtained often provide the information necessary to unravel the energy-band complications and reveal the effects due to interactions.

Cyclotron resonance was first observed for electrons in InSb at microwave frequencies by Dresselhaus, Kip, Kittel, and Wagoner.[8] These results showed that the conduction band is at the center of the zone and has an effective mass $\approx 0.013m$. Observations at infrared frequencies were originally made at Lincoln Laboratory[9] and at NRL.[10] These results showed that the conduction band could not be described by an effective mass independent of energy (magnetic field). Structure due to impurities was first observed by Boyle and Brailsford.[11] The role of electron-phonon interaction in shifting Landau levels was first demonstrated by Johnson and Larsen[2] in interband magnetoabsorption and subsequently in cyclotron resonance by Dickey, Johnson, and Larsen.[3]

Cyclotron-resonance-like transitions involving an apparent spin flip have been observed by the NRL group[12] and by Dickey and Larsen.[4] Oscillations in the free-carrier absorption at higher energies than those normally associated with cyclotron resonance have been observed by Palik and Wallis.[13] We have observed such absorption over a wide range of energy and magnetic field and have identified these transitions as harmonics of cyclotron-resonance and phonon-assisted harmonics of cyclotron resonance in a preliminary report.[14] We discuss the cyclotron-resonance harmonics and phonon related transitions more completely in this paper. Fan and co-workers have independently observed and identified absorption involving phonon-assisted harmonics of cyclotron resonance.[15]

II. EXPERIMENTAL PROCEDURE

The experimental results were obtained by observing the infrared transmission of InSb samples versus magnetic field for fixed wavelengths from 28 to 275 μ (44 to 4.5 meV). The monochromator used was a vacuum $f/4$ Czerny-Turner grating monochromator built in this laboratory with special features to enhance resolution. Precautions were taken to avoid strain in the samples. A selection of sample temperatures was used so that in a given run either free-carrier or impurity absorption would predominate.

Monochromator

A schematic drawing of the monochromator is shown in Fig. 1. The dispersion elements (located at G) were $7\frac{1}{2}\times 8$ in. gratings having 15-deg blaze angles. Rejection of unwanted higher-order radiation was accomplished using a variety of filters listed in Table I. They include echlette reflection filters and crystal reststrahlen filters. The transmission filters were mounted in the detector light pipe. Additional purification was obtained by using a crystal chopper.

Off-axis aberrations were corrected to first order by using cylindrical mirrors of slight curvature in place of conventional plane mirrors at the positions C in the figure. As a result a sharp image of the source is obtained at the entrance slit and sharp images of the exit slit are obtained at the sample position and at the detector. A 100-W mercury arc is used as the infrared source located at B in the drawing. Higher-power sources, which merely compensate for aberrations, are often used. That this was unnecessary in our case, was demonstrated by substituting a 1000-W mercury arc in place of our 100-W source. No improvement in signal was obtained even with the slit width set at 6 mm, which was 80% of the 100-W arc width.

To avoid unnecessary attenuation of the signal, the optical path is completely enclosed in vacuum with no windows except for two of clear polyethylene at the detector position, one on the detector Dewar and one on the exit port of the spectrometer (w in the figure for the transmission arrangement, w′ for reflection). These windows allow a separation of 8 mm between the detector Dewar and the spectrometer. This provides a space into which transmission filters and polarizers may be placed.

[7] R. A. Isaacson, Phys. Rev. **169**, 312 (1968); for earlier work see G. Bemski, Phys. Rev. Letters **4**, 62 (1960).
[8] G. Dresselhaus, A. F. Kip, C. Kittel, and G. Wagoner, Phys. Rev. **98**, 556 (1955).
[9] B. Lax, J. G. Mavroides, H. J. Zieger, and R. J. Keyes, Phys. Rev. **122**, 31 (1961).
[10] E. D. Palik, G. S. Picus, S. Teitler, and R. F. Wallis, Phys. Rev. **122**, 475 (1961).
[11] W. S. Boyle and A. D. Brailsford, Phys. Rev. **107**, 903 (1957).
[12] B. D. McCombe, S. G. Bishop, and R. Kaplan, Phys. Rev. Letters **18**, 748 (1967).
[13] E. D. Palik and R. F. Wallis, Phys. Rev. **130**, 41 (1963).
[14] D. H. Dickey and E. J. Johnson, Bull. Am. Phys. Soc. **13**, 430 (1968).
[15] H. Y. Fan, in Proceedings of the International Conference on Physics of Semiconductors, Moscow, 1968, p. 135 (unpublished).

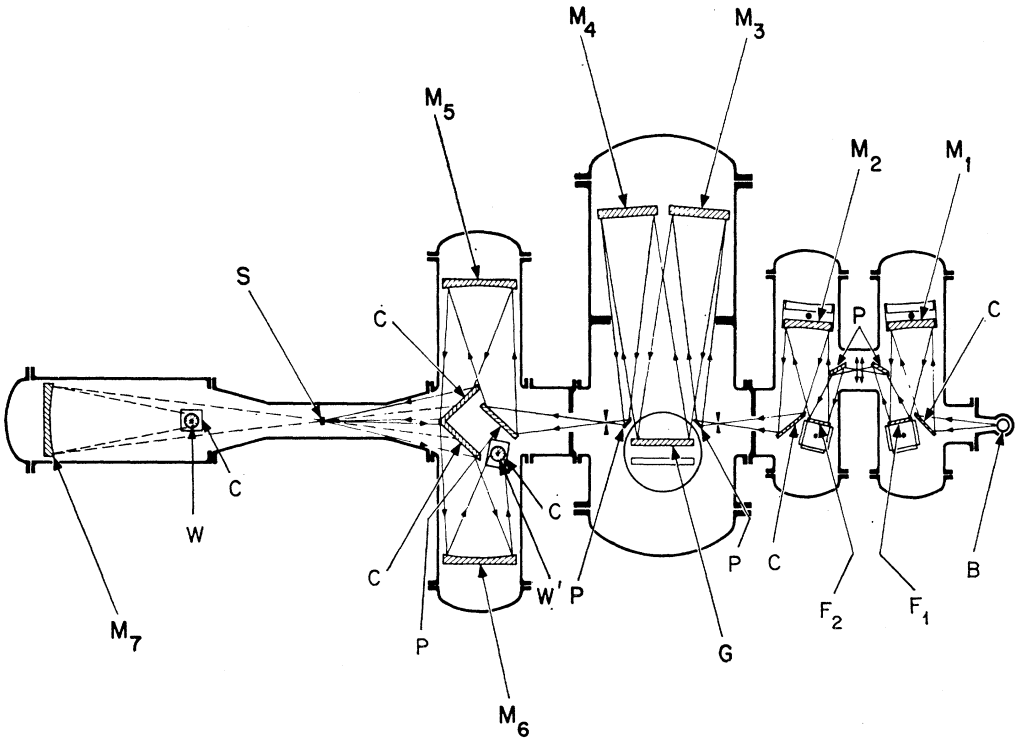

Fig. 1. Optical path of spectrometer.

Detector

An indium-doped germanium bolometer detector at approximately 1.5°K served as the detector. This particular material, grown by the General Electric Co., had $A=11.6$°K and $\rho(300°\text{K})=0.07$ Ω cm. (A characterizes the resistance of bolometer material in the neighborhood of the operating temperature and is defined in terms of the bolometer resistance by $R=R_0e^{A/T}$.) This large value of A may account for the low NEP obtained.

The electrical signal is developed across a 1-M Ω resistor in series with the 100 000- to 200 000-Ω detector and a 6.75-V battery. A Princeton model HR-8 synchronous amplifier and a Minneapolis-Honeywell Brown strip chart recorder completed the electrical system.

Magnet

The sample was located at position S in the drawing. Magnetic fields up to 35.5 kG were provided using a 9-in. Varian magnet. The pole tips of the magnet were an integral part of the vacuum chamber which provided a common vacuum for the spectrometer and the sample Dewar. This procedure eliminates Dewar windows and allows the air gap in the magnet to be minimized. The

TABLE I. Filters.

Range (μ)	Grating blaze	Crystal chopper	Reflection filters		Ruled sphere[a]		Transmission filter
			F_1	F_2	M_1	M_2	
28–40	44	NaCl	NaF	Scatter plate[b]	1760	600	1-mm sapphire (~1.5°K), black polyethylene
35–60	44	KBr	NaCl	Scatter Plate[b]	600	330	1-mm sapphire (~1.5°K), black polyethylene
50–100	78	KBr	NaCl KCl KBr	300[c]	600	330	1-mm sapphire (~1.5°K), black polyethylene
100–200	132	CsI	KI CsBr	300[c]	330	113	1-mm sapphire (~1.5°K), black polyethylene
140–300	207	KBr	250 mesh[d]	250 mesh[d]	330	113	1-mm sapphire (~1.5°K), black polyethylene

[a] Focusing echlette filters, specified in lines per in. at 15°K blaze angle.
[b] Ground aluminum flat.
[c] Flat ruled echlette filter, blazed at 15°.
[d] Woven beryllium-copper wire mesh filters.

magnetic field was measured by a Hall probe mounted on a pole tip of the magnet. The magnetic field was oriented perpendicular to the propagation of the radiation and parallel to a ⟨110⟩ crystal direction. Linearly polarized radiation was obtained using a polyethylene wire grid polarizer.

Samples

Experimental results for absorption near the fundamental cyclotron resonance were obtained using InSb samples of approximately 20-μ thickness prepared from n-type material ($n_{77°K}\approx 10^{14}$ cm^{-3} and $\mu_{77°K}\approx 6\times 10^5$ cm^2/V sec). For measurements in the region of the harmonics and phonon-assisted harmonics, Te-doped samples of thickness ~ 2 mm with $n\approx 1.4\times 10^{15}$ cm^{-3}, $\mu_{77°K}=3\times 10^5$ (cm^2/V sec) were used.

Measurements were made in a range of sample temperatures between about 10 and 60°K. A selection of temperatures was obtained by varying the thickness of a sheet of Mylar which thermally insulated the sample from a heat sink at helium temperature. To avoid strain upon cooling, the thin InSb sample was first secured to a thick piece of InSb with a suitable slit through which the radiation transmitted by the sample could pass. This package was attached at one end to a sample holder of molybdenum.

The question has been raised of whether or not the reflectivity could affect the conclusions obtained in this work. We have assumed that the reflectivity is flat in the neighborhood of the resonance and that the peak observed in transmission coincides with the peak in absorption which gives the energy-level separation at a given magnetic field. For the low-level absorption involving the cyclotron-resonance harmonics and the phonon-assisted transitions this assumption is justified, and for the low-carrier-concentration samples we have used it is correct for the fundamental cyclotron resonance. At some higher concentration, structure in the reflectivity (see Ref. 9) might shift the position of the transmission peak. However, the shift is always less than a small fraction of a linewidth which in our case would produce an uncertainty of about 2%, which is on the order of other uncertainties present, and could not affect any of the conclusions.

III. THEORY OF ENERGY LEVELS

We summarize the expressions needed to calculate the magnetic energy levels and to fit theoretical expressions to the observed transition energies.

The Hamiltonian for an electron in InSb in the presence of a magnetic field (H) can be written

$$(\mathbf{P}^2/2m+V_0+H_{e,l}+V_{\text{imp}}), \tag{1}$$

where $\mathbf{P}=\mathbf{p}+(e/c)\mathbf{A}$, $\mathbf{A}=\frac{1}{2}\mathbf{H}\times\mathbf{r}$. The first term is just that for a free electron in a magnetic field. The second term gives the interaction with the crystal periodic potential. The third and fourth terms give the interaction between the electron and the lattice, and between the electron and impurities, respectively. We first consider the effect of the crystal potential and separately examine the perturbation imposed by the electron-lattice interaction and that due to impurities.

The theory of the magnetic energy levels in the conduction band of InSb has been treated by Lax *et al.*[9] and by Bowers and Yafet.[16] The perturbation imposed by the magnetic field is handled by applying the Luttinger-Kohn[17] effective-mass theory to the zero-field results. Here we use a Wigner-Brillouin decoupling procedure to obtain coupled equations for a subset of bands.[18]

The energy levels near the bottom of the conduction band of InSb have been treated theoretically by Kane.[19] The wave functions have s-like symmetry near $k=0$ and the energy surfaces are nearly spherical. The energy levels are given by

$$E_c(k)=\hbar^2k^2/2m^*, \tag{2}$$

where m^* is an energy-dependent effective mass and is a scalar in the spherical approximation, which is given in Wigner-Brillouin perturbation theory by

$$\frac{m}{m^*}=1+\frac{1}{m}\sum_{l\neq c}\frac{|p_{cl}{}^x|^2}{E_c(k)-E_l(0)}, \tag{3}$$

where the summation is taken over all energy bands l with energy at $k=0$ of $E_l(0)$, and where $p_{cl}{}^\eta$ is the η component of the momentum matrix element between bands c and l at $k=0$.

For energy bands far removed in energy from the conduction band, the effect of the difference between $E_c(k)$ and $E_c(0)$ in Eq. (3) is small, and we can write

$$\frac{m}{m^*}\approx 1+\frac{m}{m_{\text{rb}}}+\frac{2}{m}\sum_{\text{val band}}\frac{|p_{cl}{}^x|^2}{E_c(k)-E_l(0)}, \tag{4}$$

where the effect of the remote bands is concentrated in the term m/m_{rb}, where the energy dependence is neglected.

In InSb the valence band is p-like and is split at $k=0$ by the spin-orbit interaction energy Δ. Substitution of (4) into Eq. (2) gives a cubic equation for the energy $E_c(k)$. The solution relevant to the conduction band can be written

$$E_c(k)=-\tfrac{1}{2}E_g+\tfrac{1}{2}(\hbar^2k^2)\left(\frac{1}{m}+\frac{1}{m_{\text{rb}}}\right)+\tfrac{1}{2}E_g\left(1+4\frac{\hbar^2k^2}{2m_c}\frac{f_1(E_c)}{E_g}\right)^{1/2}, \tag{5}$$

[16] R. Bowers and Y. Yafet, Phys. Rev. **115**, 1165 (1959).
[17] J. M. Luttinger and W. Kohn, Phys. Rev. **97**, 869 (1955).
[18] We are indebted to H. J. Zeiger for access, before publication, to a detailed discussion of this procedure in his book with G. W. Pratt (unpublished). See also Ref. 9.
[19] E. O. Kane, J. Phys. Chem. Solids **1**, 249 (1957).

where m_c is defined at $E_c(k)=0$ by

$$1/m_c=1/m^*-1/m-1/m_{\rm rb}. \tag{6a}$$

It is given in the present case by

$$\frac{m}{m_c}=\frac{2}{m}|\langle s|p_z|z\rangle|^2\frac{E_g+\frac{2}{3}\Delta}{E_g(E_g+\Delta)}. \tag{6b}$$

The quantity $f_1(E_c)$ is equal to unity at $k=0$ and is weakly energy-dependent:

$$f_1=\frac{(E_g+\Delta)(E_c(k)+E_g+\frac{2}{3}\Delta)}{(E_g+\frac{2}{3}\Delta)(E_c(k)+E_g+\Delta)}. \tag{7}$$

In considering the effect of an applied magnetic field, we must take explicit account of the fact that the conduction-band edge is twofold degenerate. Although electron spin is mixed owing to spin-orbit interaction, Kramer's theorem[18] must apply giving, for example, the wave functions for the pair of degenerate levels at $k=0$:

$$\begin{aligned}u_{c,0}^{(\uparrow)}&=u_{c,0}^{(\alpha)}(r)\begin{pmatrix}1\\0\end{pmatrix}+u_{c,0}^{(\beta)}(r)\begin{pmatrix}0\\1\end{pmatrix},\\ u_{c,0}^{(\downarrow)}&=-u_{c,0}^{(\beta)*}(-r)\begin{pmatrix}1\\0\end{pmatrix}+u_{c,0}^{(\alpha)*}(-r)\begin{pmatrix}0\\1\end{pmatrix},\end{aligned} \tag{8}$$

where the parentheses indicate matrices.

In the presence of a magnetic field, the conduction-band wave functions are modified and become to first order

$$\begin{aligned}\psi_{c,j}^{(\uparrow)}&=f_{c,j}^{(\uparrow)}(r)u_{c,0}^{(\uparrow)}+f_{c,j}^{(\downarrow)}(r)u_{c,0}^{(\downarrow)},\\ \psi_{c,j}^{(\downarrow)}&=f_{c,j}^{(\uparrow)}(r)u_{c,0}^{(\uparrow)}-f_{c,j}^{(\downarrow)}(r)u_{c,0}^{(\downarrow)},\end{aligned} \tag{9}$$

where the subscript j indicates any member of the set of perturbed conduction-band states and the f's are solutions of the pair of coupled equations obtained by applying Luttinger-Kohn effective-mass theory. The coupled equations can be expressed in matrix notation by

$$\left(\frac{\mathbf{P}^2}{2m}\mathbf{I}+\sum_\mu\frac{\mathbf{P}\cdot\mathbf{p}_{c\mu}\mathbf{p}_{\mu c}\cdot\mathbf{P}}{E_{c,j}-E_\mu(0)}+2\beta\mathbf{S}_c\cdot\mathbf{H}-E_{c,j}\mathbf{I}\right)\begin{pmatrix}f_{c,j}^{\uparrow}\\f_{c,j}^{\downarrow}\end{pmatrix}=0. \tag{10}$$

The magnetic energy levels are given by the eigenvalues $E_{c,j}$. In Eq. (10), $\mathbf{p}_{c\mu}$ and $\mathbf{S}_c$ are the matrix vectors

$$\mathbf{p}_{c\mu}=\begin{pmatrix}\mathbf{p}_{c\uparrow\mu\uparrow}&\mathbf{p}_{c\uparrow\mu\downarrow}\\ \mathbf{p}_{c\downarrow\mu\uparrow}&\mathbf{p}_{c\downarrow\mu\downarrow}\end{pmatrix}, \tag{11}$$

$$\mathbf{S}_c=\begin{pmatrix}\mathbf{S}_{c\uparrow c\uparrow}&\mathbf{S}_{c\uparrow c\downarrow}\\ \mathbf{S}_{c\downarrow c\uparrow}&\mathbf{S}_{c\downarrow c\downarrow}\end{pmatrix}, \tag{12}$$

where $\mathbf{S}_{c\uparrow c\uparrow}$, etc., are the appropriate matrix elements of the Pauli spin operator $\mathbf{S}$.

The effect of the real electron spin is given by the third term in (10) and corresponds to a g factor of $+2$. Roth has shown that the evaluation of the second term in a magnetic field yields a magnetic moment that behaves very much like the normal electron spin, given by the third term. Equation (10) can be written

$$[(\mathbf{P}^2/2m^*)\mathbf{I}+\beta g^*\mathbf{S}\cdot\mathbf{H}-E_{c,j}\mathbf{I}]\mathbf{f}_{cj}(r)=0, \tag{13}$$

where the energy-dependent effective mass m^* is the same as with $H=0$ and g^* is the energy-dependent g factor given by

$$g^*(F_{c,j})=2-\frac{2}{mi}\sum_{l\neq c}\frac{p_{cl}^x p_{lc}^y-p_{cl}^y p_{lc}^x}{E_{c,j}-E_l(0)}, \tag{14}$$

or by analogy with Eq. (4)

$$g^*(E_{c,j})=2+g_{\rm rb}-\frac{2}{mi}\sum_{\text{val band}}\frac{p_{cl}^x p_{lc}^y-p_{cl}^y p_{lc}^x}{E_{c,j}-E_l(0)}, \tag{15}$$

where $g_{\rm rb}$ is the remote-band contribution to the g factor. Further, Roth, Lax, and Zwerdling[20] have shown that m^* and g^* for conduction and valence bands like InSb or germanium are related. We generalize this result using (4) and (15) to include remote bands, giving

$$\frac{m/m^*-1-m/m_{\rm rb}}{g^*-2-g_{\rm rb}}=-\tfrac{2}{3}E_g/\Delta+1. \tag{16}$$

Equation (15) can be handled most easily if the free-electron and remote-band terms in Eqs. (4) and (15) are treated as small perturbations. Solutions can then be obtained in terms of the usual Landau level wave functions and one obtains a cubic equation for the energy eigenvalues. The solution relevant to the conduction band can be written

$$E_{n\pm}=-\tfrac{1}{2}E_g+\tfrac{1}{2}E_g\left[1+\frac{4f_1}{E_g}\times\left((2n+1)\frac{m}{m_c}\beta H\pm\tfrac{1}{2}g\beta Hf_4+\frac{\hbar^2k_z^2}{2m_c}\right)\right]^{1/2}, \tag{17}$$

where g is the band-edge value of $(g^*-2-g_{\rm rb})$. The function f_4 is given by

$$f_4=(E_g+\tfrac{2}{3}\Delta)/(E_{n\pm}+E_g+\tfrac{2}{3}\Delta). \tag{18}$$

An additional term $E_{n\pm}'$ due to free-electron and remote-band contributions should be added to the right-hand side of (17). This term can be expected to shift the energy levels and to affect the spin splitting. It is convenient in comparing the theory with experi-

[20] L. M. Roth, B. Lax, and S. Zwerdling, Phys. Rev. 114, 90 (1959).

ment to take this term into account approximately,[21] by taking for $1/m_c$ the value

$$\frac{1}{m_c'}=\frac{1}{m}+\frac{1}{m_{\rm rb}}+\frac{1}{m_c}, \tag{19}$$

and for g,

$$g'=2+g_{\rm rb}-2\frac{m}{m_c}\frac{\Delta}{3E_g+2\Delta}. \tag{20}$$

With magnetic energy levels having the form of Eq. (17), we can expect the cyclotron resonance for InSb to depart from the normal behavior in several ways: (a) The cyclotron-resonance energy will not be linear with magnetic field; (b) the magnitude of the cyclotron-resonance energy at a given value of H will depend upon the value of n in the ground state; and (c) the cyclotron-resonance energy for spin up will be different from that for spin down.

Electron-Phonon Interaction

We have observed transitions that result from electron-phonon interaction. Below we show how such an interaction can affect the selection rules. We can also expect polaron self-energy effects to shift the energy levels. With a coupling constant (see below) of 0.02 for InSb the polaron self-energy effects on the cyclotron-resonance energy can be shown to be negligibly small over a wide range of magnetic field. However, as has been shown theoretically and confirmed experimentally, the polaron self-energy effects[2-4] can become strongly enhanced near magnetic fields where the zero-phonon energy levels would cross the one-phonon energy levels, even in the case of low coupling constant. In the analysis of the experimental results one must be alert for such localized effects.

Impurity Interaction

At $H=0$ the donor impurity states in InSb are degenerate with the conduction-band levels, principally owing to the very low electron effective mass. With application of magnetic field the diamagnetic effect separates impurity states from each of the Landau levels.[22] The energy separation between the lowest impurity state associated with a given Landau level and the given Landau level we refer to as the impurity ionization energy of the given Landau level. In a high magnetic field the impurity ionization energy varies slowly with magnetic field and decreases rapidly with Landau quantum number.[23]

[21] If $\hbar^2k^2/2m_2\ll\hbar^2k^2/2m_1\ll E_g$, it is a good approximation that $\frac{1}{2}E_g[1+(4/E_g)(\hbar^2k^2/2m_1)]^{1/2}+\hbar^2k^2/2m_2 \approx\frac{1}{2}E_g[1+(4/E_g)\frac{1}{2}(\hbar^2k^2)(1/m_1)+1/m_2]^{1/2}$.

[22] Y. Yafet, R. W. Keyes, and E. N. Adams, J. Phys. Chem. Solids **1**, 137 (1956); R. F. Wallis and H. J. Bowlden *ibid.* **7**, 78 (1958).

[23] R. J. Elliott and R. Loudon, J. Phys. Chem. Solids **15**, 196 (1959).

The impurity levels can be obtained as solutions of the effective-mass equation

$$[E_c(\mathbf{p}+e\mathbf{A}/c)-e/\kappa r]\psi_n=E_n\psi_n. \tag{21}$$

For a parabolic band $E=\hbar^2k^2/2\mu$, where μ is a constant effective mass; and setting $\mathbf{A}=\frac{1}{2}\mathbf{H}\times\mathbf{r}$ this can be written

$$R\left[-a^2\nabla^2-\frac{1}{2}\frac{a}{r}+\frac{\gamma}{i}\frac{\partial}{\partial\phi}+\frac{1}{4}\left(\frac{r^2}{a^2}\sin^2\theta\right)\gamma^2\right]\psi_n=E_n\psi_n, \tag{22}$$

with R and a related to the hydrogen Rydberg constant R_0 and Bohr radius a_0 by

$$R=(\mu/m)(1/\kappa^2)R_0, \quad a=\kappa(m/\mu)a_0. \tag{23}$$

Here κ is the static dielectric constant, and γ is a variable proportional to magnetic field, i.e.,

$$\gamma=\tfrac{1}{2}\hbar\omega_c/R. \tag{24}$$

For $\gamma\gtrsim1$, the usual hydrogen atom solutions obtained for low fields are no longer valid, since states of the same parity and magnetic quantum number become mixed and one must resort to variational calculations for the energy levels. Larsen[24] has used the following trial wave functions in a variational calculation to obtain the lowest state with even parity $M=0$, and with odd parity, $M=\pm1$:

$$e^{-\rho^2/Q^2}e^{-S(\rho^2+TZ^2)^{1/2}}, \quad M=0 \tag{25a}$$

$$\rho e^{-\rho^2/Q^2}e^{-S(\rho^2+TZ^2+V^2)^{1/2}}e^{\pm i\phi}, \quad M=\pm1, \tag{25b}$$

where the variables are cylindrical coordinates and Q, S, and U are adjusted to minimize the energy independently for each function and each magnetic field.

The optical transition involving these states corresponds roughly to the $1s$-$2p$ hydrogen atom transition. At high fields, the energy separation between the levels ($M=0$ and $M=+1$) is approximately equal to the separation of the first two Landau levels (0+ and 1+). Experimentally, it is convenient to measure the energy separation δ between the relevant cyclotron-resonance transition and the impurity transition. Theoretically, this energy separation should be

$$\delta=(E_{I,M=+1}-E_{I,M=0})-(E_{1+}-E_{0+}). \tag{26}$$

This quantity has been calculated by Larsen[24] who has also considered nonparabolic band effects. The results are reproduced below.

IV. EXPERIMENTAL RESULTS FOR CYCLOTRON-RESONANCE AND DETERMINATION OF BAND-EDGE PARAMETERS

Effective Mass

We use the cyclotron-resonance results to obtain a precise determination of the band-edge effective mass

[24] D. M. Larsen, J. Phys. Chem. Solids **29**, 271 (1967).

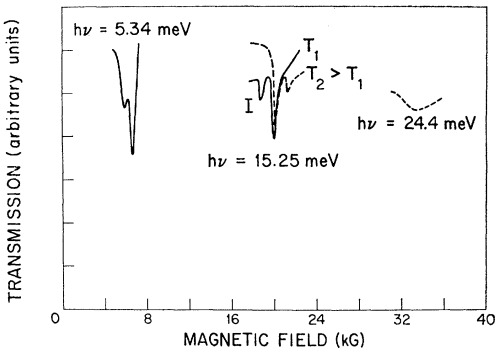

FIG. 2. Cyclotron-resonance spectra observed in thin samples ($t \approx 20\ \mu$) at temperatures near liquid helium such that $T_2 > T_1$.

and to check the fit of the experimental results to the nonparabolic theory. It is important in doing this to carefully note and to take into account effects due to impurities and effects due to electron-phonon interaction.

In Fig. 2 we show experimental traces of sample transmission versus magnetic field at certain fixed photon energies below and above the reststrahl energy. These samples are $\approx 20\ \mu$ in thickness and reveal only the strong absorption near $\hbar\omega_c$. Near the range $\hbar\omega_{TO} < h\nu < \hbar\omega_{LO}$, the sample is opaque owing to high reststrahl reflection. In Fig. 2, we see that the absorption, in general, involves three peaks whose relative strengths depend upon temperature. The three peaks are not resolved[3] for $h\nu > \hbar\omega_{LO}$.

The absorption peak due to impurity transitions can be identified by two considerations: (a) It should lie at higher energies (lower H at fixed energy) than the free-electron transitions, and (b) the impurity transition should be absent at higher temperatures, becoming prominent at lower temperatures. This behavior is followed by the peak labeled I in Fig. 2.

The remaining two peaks are evidently free-electron cyclotron resonance where the spin degeneracy has been removed by nonparabolic effects. This identification is confirmed by the temperature behavior of the relative strengths of the two peaks (i.e., the peak that occurs at lower energy is the one that disappears at lower temperatures). Measurements were also made on samples with higher carrier concentration. In these samples, the absorption lines broaden and obscure the distinction between impurity absorption and free-carrier absorption.

The experimentally observed cyclotron-resonance energies are plotted versus magnetic field in Fig. 3. The anomalous behavior at higher energies is due to polaron effects and has been described in detail previously.[3] The decrease in slope of $h\nu_{CR}$ versus H in approaching the reststrahl region from below is partly due to the nonparabolic nature of Eq. (17) and partly due to polaron effects.[4] The polaron effect, however, dies out very quickly as the photon energy decreases below the reststrahl region. Theoretically this should be the case,[2] and is demonstrated quite well in the least-squares fit of the data to the energy-level separations calculated using Eq. (17). If all of the data are used, one obtains a relatively large mean-square deviation indicating a poor fit. As one removes the high-energy data points in sequence in going to lower and lower energy, the mean-square deviation obtained in the fit becomes significantly smaller until all points above $h\nu_{CR} \approx 18$ meV have been removed. Further removal of data points does not significantly alter the mean-square deviation. The final fit was obtained using only the data points below 18 meV.

In obtaining the fit to the data, one has two adjustable parameters m_c' and g'. Since the g factor plays a role in cyclotron resonance only via the nonparabolic effects, it should not be surprising that the fit is insensitive to the precise choice of the magnitude of g' between values of 40–70. A choice of g' in this range results in only a slight uncertainty in the value of m_c'. We obtain a value of $m_c' = 0.0189m \pm 0.0001m$ for the band-edge effective mass in Insb. This value of m_c'/m conflicts with the value of 0.0149 ± 0.0005 obtained by the Pidgeon-Brown[5] type of analysis of *interband* absorption.[25] However, as will be shown below, the values of m_c' obtained in the various *intraband* experiments are quite consistent.

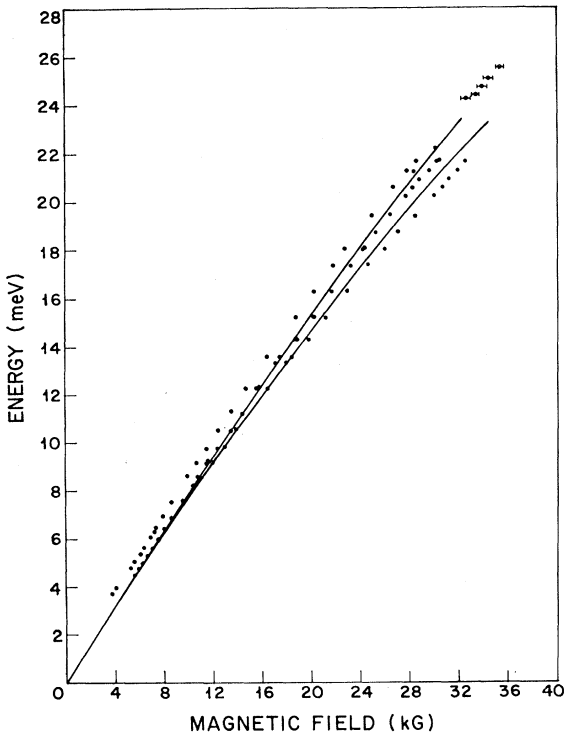

FIG. 3. Variation of cyclotron-resonance absorption peaks with magnetic field. The solid lines give the theoretical predictions for spin-up and spin-down transitions, respectively, using $m_c' = 0.139$ and $g' = -51.3$.

[25] C. R. Pidgeon and S. H. Groves (unpublished).

The theoretical fit to the data is shown in Fig. 3. A value of $g'=-51.3$ is used in anticipation of the results of experiments to be discussed below.

g Factor

Spin-resonance experiments of Isaacson[7] for a sample with $n=3.6\times10^{13}$ cm^{-3} and $H\approx0.5$ kG yield an experimental g factor of 51.3 ± 0.1. Such a sample would have a Fermi level $\zeta\approx0.3$ meV and should yield a value very close to the band-edge value.

To check the ability of Eq. (17) to predict the experimental spin energy at higher magnetic fields, we have (a) analyzed combination resonance measurements which observe the transition E_{0+} to E_{1-} (this involves a spin flip[4]), and (b) have analyzed Isaacson's spin-resonance data for higher carrier concentrations, which involves higher Landau levels. We discuss the combined resonance results immediately, but defer the discussion of the spin-resonance results until later in the paper.

The shift of the combined resonance absorption peaks with magnetic field is shown in Fig. 4 and compared to calculations of the energy E_1-E_{0+} according to Eq. (17) and a value of $g'=-51.3$. Excellent agreement between experiment and theory is obtained for magnetic fields less than ~27 kG. The deviation between experiment and theory above 27 kG coincides with the anomalous region observed in straight cyclotron resonance and is easily attributed to the polaron self-energy effect. Therefore, we conclude that the value of -51.3 for the band-edge g factor is a good one, and that Eq. (17) faithfully predicts the spin energy for fields up to 27 kG.

Equation (16) gives the relationship between the g factor and the effective mass for InSb. Using $E_g=236.7\pm0.2$ meV (Ref. 26) and $\Delta=810\pm10$ meV (Ref. 27) we have

$$\frac{70.9\pm0.5-m/m_{\rm rb}}{53.3\pm0.1+g_{\rm rb}}=1.44\pm0.01.$$

The ratio of the numbers on the left is 1.33 ± 0.01. This indicates that $m/m_{\rm rb}$ and $g_{\rm rb}$ are not both zero. If $g_{\rm rb}=0$, then $m/m_{\rm rb}=-5.9$. On the other hand, if $m/m_{\rm rb}=0$, then $g_{\rm rb}=-4.1$.

The momentum matrix element $P^2=(2/m)|\langle s|p_z|z\rangle|^2$ is related to the effective mass by Eq. (6). Considering the uncertainty in m/m_c, we obtain $P^2=24\pm1$ eV (0.44 ± 0.02 a.u.).

V. IMPURITY TRANSITIONS

The third absorption peak of Fig. 2 is apparently an impurity transition. The shift of this peak with magnetic field is qualitatively similar to the shift of the cyclotron-resonance peaks. However, whereas the energy of the cyclotron-resonance peaks extrapolates to zero at $H=0$, the energy of the impurity peaks extrapolates to a value on the order of 0.3 meV. The separation in energy between the impurity peak and the low-temperature cyclotron-resonance peak as a function of magnetic field is shown in Fig. 5. The theoretical values of δ, calculated by Larsen[24] using $R=0.6$ meV, is also plotted and compared to the experimental results. From 8–25 kG, the data agree qualitatively with the theory except that a larger value of R would appear to give a better fit. This discrepancy should not be taken as placing in doubt the values of effective mass and static dielectric constant used. The discrepancy is more likely due to the failure of effective-mass theory to give a good value for the energy of the ground state, which is s-like in character and, therefore, can be expected to be affected strongly by central-cell effects. One might suggest that the discrepancy is due to nonparabolic effects, since the higher effective masses at higher magnetic fields would give higher ionization

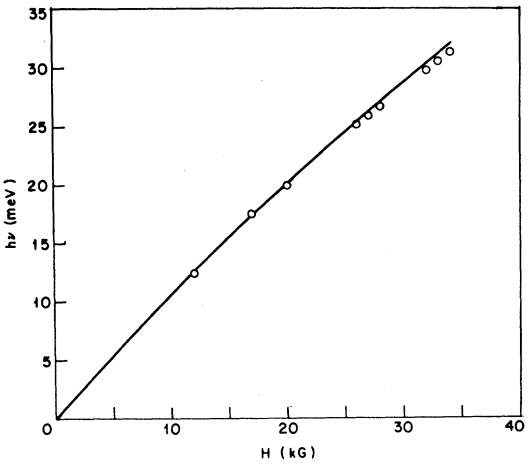

FIG. 4. Variation of combination-resonance peaks with magnetic field. The solid line gives the theoretical prediction.

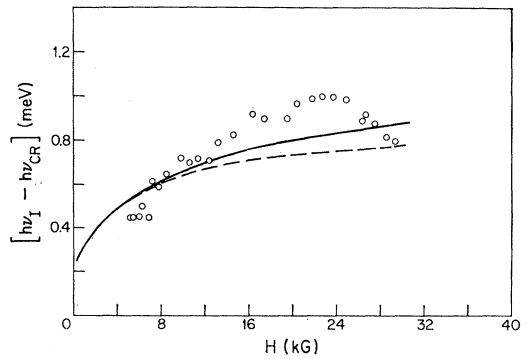

FIG. 5. Comparison of the splitting $h\nu_I-h\nu_{\rm CR}$ with theoretical predictions: solid line, parabolic band theory; dashed line, nonparabolic theory.

[26] E. J. Johnson, Solid State Research Report No. 4, Lincoln Laboratory, MIT 1967, p. 33 (unpublished); and (unpublished).
[27] C. R. Pidgeon, S. H. Groves, and J. Feinleib, Solid State Commun. **5**, 677 (1967); R. L. Aggarwal, Bull. Am. Phys. Soc. **12**, 100 (1967).

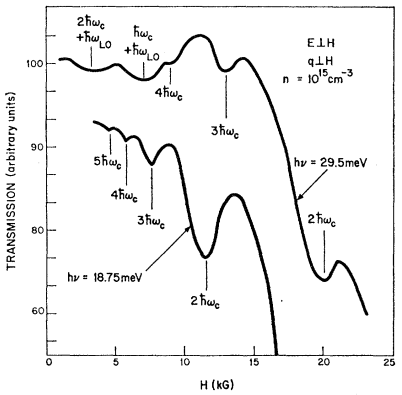

FIG. 6. Cyclotron-resonance spectra observed in thick samples ($t \approx 2$ mm) with radiation polarized $E \perp H$.

energies. Larsen's theory including effects due to nonparabolic bands (Fig. 6) shows, however, that the energy separation δ actually decreases from that predicted by parabolic theory.

More interesting is the decrease of δ with increasing H for magnetic fields greater than 25 kG. This behavior is in contrast with the monotonic increase of δ with increase in H predicted by the theory.[28]

We suggest that polaron effects on the higher-energy impurity level are responsible for this decrease in δ. We have seen in the cyclotron resonance and in the combined resonance transitions that the experimental separation between Landau levels falls below the value predicted by theory as magnetic field is increased above ~ 27 kG owing to resonant polaron self-energy effects. Such effects have also been observed for impurity levels in InSb.[4] The decrease in δ with increasing H observed here apparently occurs because the separation between the relevant impurity levels approaches $\hbar\omega_0$ faster than the corresponding Landau levels. As a result, the onset of pinning occurs at lower magnetic fields and proceeds faster for the impurity levels.

VI. CYCLOTRON-RESONANCE HARMONICS AND PHONON-ASSISTED TRANSITIONS

Experimental results using a thick sample $t \approx 2$ mm and $n \approx 1.4 \times 10^{15}$ m^{-3} are shown in Fig. 6. This sample thickness permits the observation of the weak absorption on the high-energy side of the fundamental cyclotron resonance. The sample temperature was near 20°K and sufficiently high to emphasize free-carrier absorption. The infrared radiation was polarized perpendicular to both the magnetic field and the propagation vector of the light. Typical magnetic field scans are shown in Fig. 6.

For $h\nu = 18.75$ meV four uniformly spaced absorption peaks are observed. The spacing is approximately equal in $1/H$ which suggests that they be identified as the second, third, fourth, and fifth harmonics of cyclotron resonance. At higher magnetic field the sample becomes opaque due to the strong absorption from the fundamental cyclotron resonance. The absorption strength decreases uniformly and relatively slowly for the higher harmonics after a drop by two orders of magnitude between the fundamental and the second harmonic. For $h\nu = 29.5$ meV, which is greater than the LO phonon energy, the uniform spacing is disturbed by the appearance of two additional absorption peaks.

The shift of the absorption peaks with photon energy is shown in Fig. 7. The peaks fall into two classes. Class 1 peaks tend to converge at $h\nu = 0$ for decreasing magnetic field; whereas, class 2 peaks tend to converge to some energy on the order of 24 meV which is close to the known value of the LO phonon energy. For a given magnetic field the energy separation between adjacent peaks is nearly constant. Such behavior would appear to support an identification of class 1 peaks as involving cyclotron-resonance harmonics and class 2 peaks as involving cyclotron-resonance harmonics and an LO phonon.

The ground states for these transitions are evidently the same as for the normal cyclotron-resonance transitions. For excited states, we have the no-phonon states $(n,0)$ given by (17) and the one-phonon states

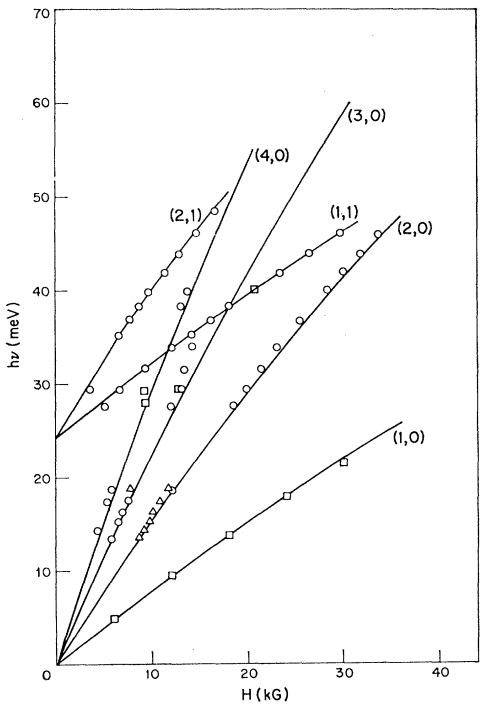

FIG. 7. Shift with magnetic field of the absorption peaks involving cyclotron-resonance harmonics and phonon-assisted transitions. The designations describe the excited states (Landau quantum number, number of phonons). The solid lines give the theoretical predictions.

[28] The nonparabolic theory of Larsen for the impurity levels does predict a maximum in δ, but such a maximum should be much broader and occur at much higher H than the maximum observed experimentally.

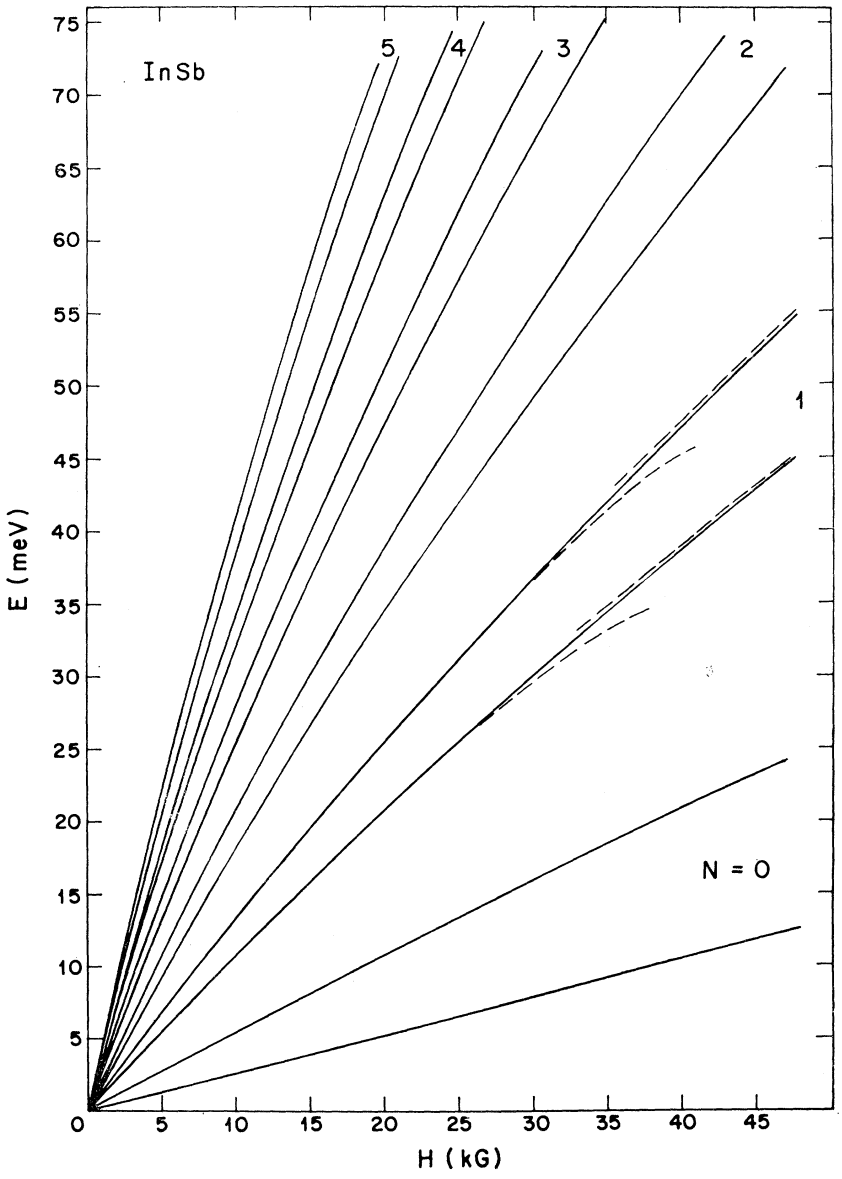

FIG. 8. Magnetic energy levels ($k_z=0$) deduced from these experiments. The energy levels have been calculated from Eq. (39) using $m_c'=0.139$ and $g'=51.3$. The dashed lines indicate the polaron corrections to the $n=1$ Landau levels.

$(n,1)$, which in first order are obtained by adding $\hbar\omega_0$ to (17).

Energy separations between the ground state and the various one-phonon and no-phonon states were calculated using the parameters given in Sec. IV. These calculations are compared to the experimental results in Fig. 7. A good agreement between experiment and theory is obtained, which confirms the identification of the transitions involved and supports the fit we have obtained between the nonparabolic theory and the observed separations between the magnetic energy levels.

In fitting the calculations to the phonon-assisted transitions $\hbar\omega_0$ occurs as an adjustable parameter. The best fit gives a value of 24.4 ± 0.3 meV for the LO phonon energy in fair agreement with other determinations.[29]

Magnetic oscillations in absorption in InSb have been reported previously and attributed to cyclotron-resonance harmonics.[13] These observations, however, were restricted to energies above 85 MeV and high magnetic fields where identification is not so easy. We have extrapolated our results to the high-field region in an attempt to identify the transitions involved in the previous results. The identification obtained is not conclusive; but it appears that the oscillations observed

[29] M. Hass, in *Semiconductors and Semimetals*, edited by R. K. Willardson and A. C. Beer, (Academic Press Inc., New York, 1967), Vol. 3, p. 11.

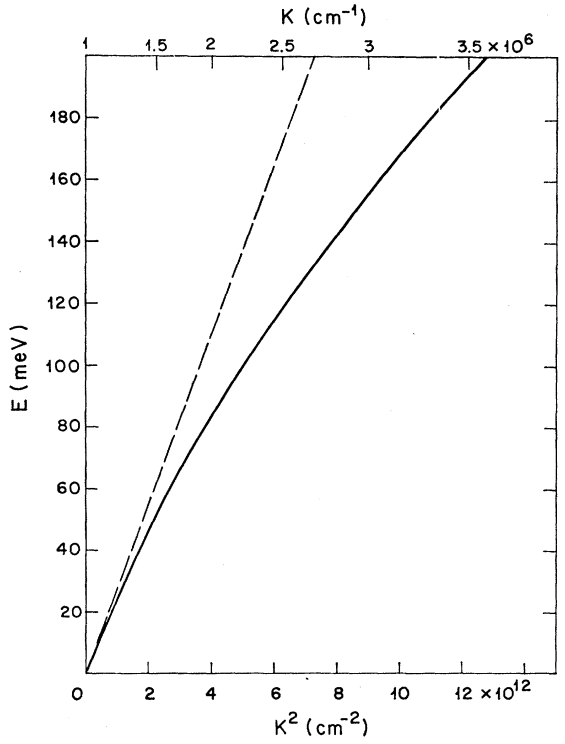

FIG. 9. Conduction-band dispersion relation deduced from these experiments. The dashed line gives the parabolic band result using band-edge value of effective mass.

previously were a mixture of cyclotron-resonance harmonics and phonon-assisted cyclotron resonance. Further work will be needed to understand the high-energy region.

It has been suggested that acoustic-phonon participation could account for the cyclotron-resonance harmonics. It would appear that this could be ruled out since: (a) Some shift would be expected due to the energy of the phonons involved. However, our analysis shows that absorption occurs at the energy predicted for the harmonics, therefore no significant shift is present. (b) The acoustic-phonon–electron interaction would be expected to be much weaker than optical-phonon–electron interaction, whereas we observe the absorption due to the harmonics to be much stronger than the absorption known to be due to optical-phonon participation.

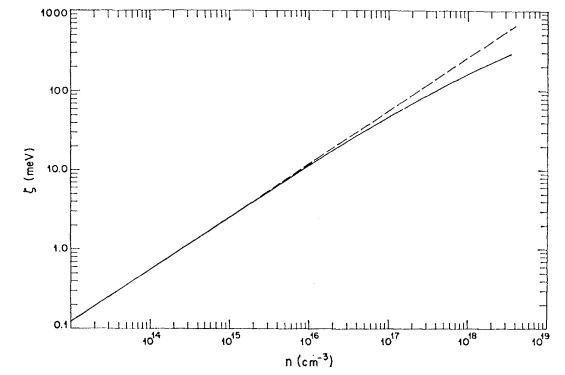

FIG. 10. Fermi level ($T=0$) versus carrier concentration for InSb as deduced from these experiments. The dashed line gives the parabolic band result.

TABLE II. Some representative values of Fermi energy and density of states versus carrier concentration.

n(cm^{-3})	ζ(meV)	$m_d(\zeta)$	$\rho(\zeta)$ (cm^{-3}/meV)
1.98×10^{13}	0.19	$0.0139m$	1.55×10^{14}
1.22×10^{14}	0.65	$0.0139m$	2.85×10^{14}
1.40×10^{15}	3.24	$0.0142m$	6.54×10^{14}
1.59×10^{16}	15.64	$0.0156m$	1.61×10^{15}
1.81×10^{17}	66.8	$0.0209m$	4.88×10^{15}
2.06×10^{18}	229	$0.0371m$	1.94×10^{16}

VII. ENERGY LEVELS DEDUCED FROM EXPERIMENTS

The variation of the magnetic energy levels with magnetic field is shown in Fig. 8. These levels were calculated using Eq. (17) and the values of m_c' and g' obtained from the fundamental cyclotron resonance and spin-flip resonance. These curves are most accurate at the lower energies. An estimation of the polaron correction to the $n=1$ Landau levels is shown dashed. The correction is calculated from theory using a coupling coefficient $\alpha=0.02$ (Ref. 2). The approximate magnitude of the effect has been confirmed by experiment.[2–4]

The accuracy of the curves for higher Landau levels to energies $\sim$60 meV has been confirmed to within 2% by the analysis of the cyclotron-resonance harmonics. The values at higher energies need further experimental confirmation.

The conduction-band energy dispersion curve is shown in Fig. 9. This is calculated using the experimental band-edge mass in Eq. (4). Confidence in the accuracy of this curve is derived from the fact that the related nonparabolic theory for the magnetic energy levels is confirmed by experiment to $\sim$60 meV. A polaron anomaly may occur at $E=\hbar\omega_c$, but is expected to be quite small.[30]

Having an energy dispersion relation for the conduction band in which one has some level of confidence permits the derivation of further quantities. In the spherical approximation, the wave vector at the Fermi level for $T=0$ is related to the carrier concentration. Therefore, the Fermi level versus carrier concentration can be obtained from the electron energy dispersion curve. This has been done and the results are given in Fig. 10. Some representative values are also given in Table II. These data are used below in analyzing the variation of spin-resonance energy with carrier concentration.

[30] D. M. Larsen, Phys. Rev. **144**, 697 (1966).

The density of states at the Fermi level can be obtained from $E(k)$ for a spherically symmetric band by

$$\rho(\zeta)=\frac{1}{\pi^2}k_\zeta^2\left(\frac{dE}{dk_\zeta}\right)^{-1}. \quad (27)$$

The result for the density of states versus energy is given in Fig. 11 and Table II.

For a simple band, the density of states can be written

$$\rho(\zeta)=\frac{1}{\pi^2}\frac{m_d}{\hbar^2}k_\zeta. \quad (28)$$

For a nonparabolic band, Eqs. (27) and (28) can be used to define an energy-dependent density-of-states mass m_d, which can be calculated from the dispersion relation. The results for InSb are shown in Fig. 12 and Table II.

The density-of-states mass, as defined, can be measured in experiments involving the susceptibility of free carriers, i.e., plasma reflectivity,[31] magnetoplasma reflectivity,[32–34] and Faraday rotation.[35] The results of such experiments for InSb, at 300 and 77°K are compared with the predicted values in Fig. 12. There is considerable scatter between the results of the various experiments, which is probably due to the fact that the experimental values represent averages over many electron states at any nonzero temperature. The spread in energy is approximately kT, i.e., ~6.5 meV at 78°K and ~25 meV at room temperature, which represents a large uncertainty in assigning an energy to the measured mass. In lieu of doing a suitable average,[35] we assign to each measured mass the energy of the $T=0$ Fermi energy obtained from Fig. 11. Considering the uncertainty in energy, the agreement between the predicted values and the experiments is quite good. It is interesting to note that the Faraday rotation results approach the predicted values with decrease in temperature. This apparently is due to less carriers high in the band (where the masses are higher) at the lower temperatures.

VIII. SPIN RESONANCE

According to Eq. (17) the size of the spin energy depends upon Landau quantum number. In a spin-resonance experiment, one can select the Landau levels whose splitting is observed, by doping the sample and moving the Fermi level through the Landau levels.

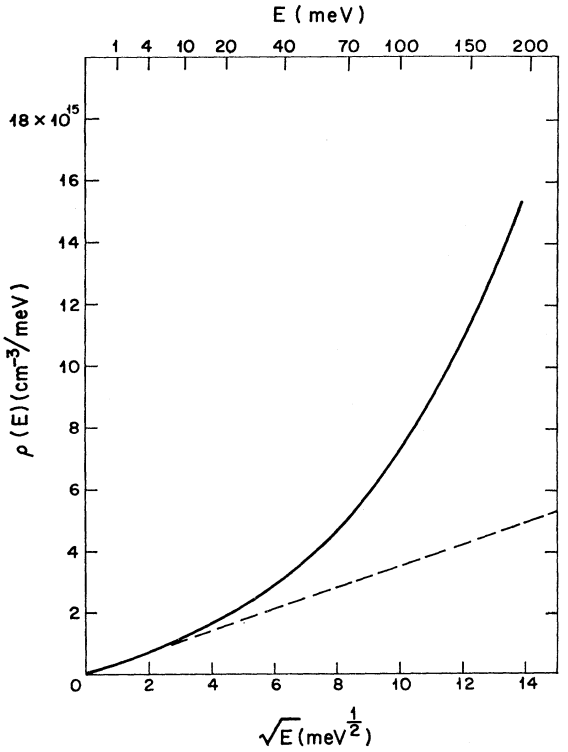

FIG. 11. Density of states versus energy. The dashed line gives the parabolic band result.

Such a spin-resonance experiment has been performed by Isaacson[7] using microwave energies of 0.037 and 0.145 meV and magnetic fields near 0.125 and 0.500 kG, respectively. With $kT\approx0.11$ meV, the spin-resonance transitions at the higher microwave energies involve at most two pairs of Landau levels. These data provide a means of checking the variations in spin energy predicted by Eq. (17). For this purpose, we define an

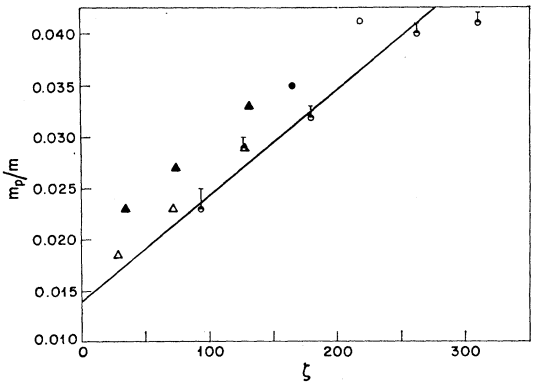

FIG. 12. Density-of-states effective mass and comparison with various experimental results. For the plasma reflection the circles give the measured values and the upward uncertainty is due to the lattice contribution (Refs. 32 and 33) to the susceptibility. Φ: plasma reflection-300°K (Ref. 31); magnetoplasma reflection-300°K. ○: Wright and Lax, Ref. 32. ●: Palik *et al.*, Ref. 34; Faraday rotation (Ref. 35). ▲: room temperature. △: 77°K.

[31] W. G. Spitzer and H. Y. Fan, Phys. Rev. **106**, 882 (1957).
[32] G. B. Wright and B. Lax, Appl. Phys. Suppl. **32**, 2113 (1961); B. Lax and G. B. Wright, Phys. Rev. Letters **4**, 16 (1960).
[33] T. S. Moss, S. D. Smith, and T. D. F. Hawkins, Proc. Phys. Soc. (London) **B70**, 776 (1957).
[34] E. D. Palik, S. Teitler, B. W. Henvis, and R. F. Wallis, in *Proceedings of the International Conference on Physics of Semiconductors, Exeter, 1962*, edited by A. C. Strickland (The Institute of Physics and The Physics Society, London, 1962), p. 288.
[35] C. R. Pidgeon, Ph.D. thesis, University of Reading, Reading, England, 1962 (unpublished).

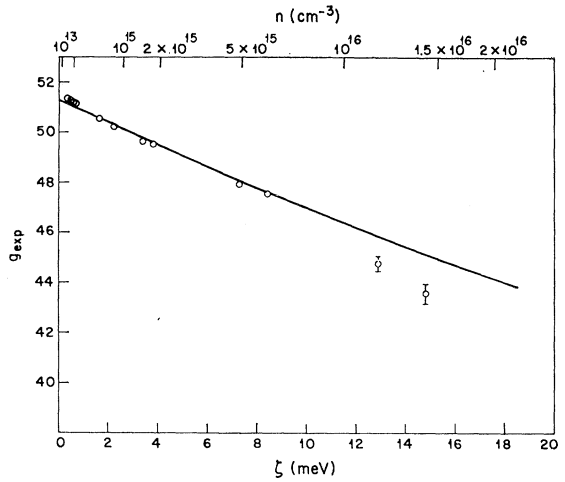

FIG. 13. Comparison of experiment and theory for variation of spin resonance with Fermi level for InSb. The experimental points are the data of Isaacson (Ref. 7) for $H\sim125$ and ~500 G. The solid line is a composite for the theoretical predictions at 0.125, 0.500, 3, and 20 kG.

experimental g factor

$$g_{\text{expt}}=h\nu_{\text{SR}}/\beta H, \tag{29}$$

where $h\nu_{\text{SR}}$ is the photon energy used in the experiment.

In Fig. 13, the solid line is our prediction of the variation of g_{expt} with Fermi level. A predicted g_{expt} was obtained for each Landau level from the spin energy calculated using (17) at a given magnetic field. This g_{expt} was assigned to a Fermi level at the average energy of the two spin levels. It is interesting that the curve in Fig. 13 is a composite of data for 0.13, 0.5, 3, and 20 kG. All points lie on the same line indicating that the g factors obtained in this way are independent of magnetic field. In Fig. 13 we also compare Isaacson's experimental data to our predictions for the variation of the spin splitting with shift in Fermi level. Excellent agreement is obtained for $\zeta\lesssim8.5$ meV, which confirms the ability of (17) to predict the spin energy.

At higher Fermi energies, a deviation occurs amounting to 5% at $\zeta\approx14$ meV. The same range in conduction-band energies is covered by the combinational resonance results where the lowest spin-down $n=0$ Landau level falls near 14 meV at 25 kG. Considering the excellent agreement in this range of conduction-band energies between experiment and theory for the combinational resonance results for a relatively pure sample, it would appear that the systematic deviation in Fig. 13 for the most impure samples may be an impurity effect.

IX. SELECTION RULES

We have observed transitions which can be attributed to cyclotron-resonance harmonics and to phonon-assisted transitions. These are both forbidden by the selection rules obtained from simple theory. In this section we reexamine the selection rules to see how these transitions might become allowed in special cases. As a first approximation we consider the transitions in a magnetic field of an electron of constant effective mass μ. We then consider the role of electron-phonon and other interactions in producing violations of the simple selection rules.

One obtains selection rules for electric dipole transitions by examining the momentum matrix element between the relevant wave functions. If the conduction-band wave functions for states i can be written as a linear combination of Bloch functions, i.e.,

$$\Phi_i=\sum_k C_i(\mathbf{k})u_{n,k}e^{i\mathbf{k}\cdot\mathbf{r}}, \tag{30}$$

the momentum matrix element between states i and j is given by[36]

$$\langle i|\mathbf{p}|j\rangle=\frac{m}{\mu}\sum_k C_i^*(\mathbf{k})C_j(\mathbf{k})\hbar\mathbf{k}. \tag{31}$$

Equation (31) requires that $\mathbf{k}$ be conserved for the transition, in the sense that for (31) to be nonzero some value of $\mathbf{k}=\mathbf{k}'$ must exist where $C_i(\mathbf{k}')$ and $C_j(\mathbf{k}')$ are both nonzero. Therefore, a necessary (but not sufficient) condition that intraband transitions occur is that a perturbation is present which mixes states of different $\mathbf{k}$. Any interaction involved in electron scattering (such as phonons, impurities, etc.) mixes electron states of different wave vector. This gives rise to the so-called free-carrier absorption, which occurs as a broad background and which can be treated by second-order perturbation theory.

In the presence of a magnetic field, states of different $\mathbf{k}$ become mixed, permitting intraband transitions. In this case, it is convenient to change Eq. (30) to the equivalent form

$$\Phi_i=u_{n,0}f_i(\mathbf{r}), \tag{32}$$

where $f_i(\mathbf{r})$ is the Fourier transform of $C_i(\mathbf{k})$ and the momentum matrix element is given by[36]

$$\langle i|\mathbf{p}|j\rangle=(m/\mu)(f_i,\mathbf{p}f_j). \tag{33}$$

For a simple parabolic band the wave functions f_i are given in cylindrical coordinates by[37]

$$f_{nMk_z}=N_{nMk_z}e^{ik_zz}e^{iM\phi}\eta^{1/2|M|}e^{-\eta/2}L_{n+|M|}^{|M|}(\eta), \tag{34}$$

where the magnetic field is in the z direction, n is a positive integer, and M is either a positive or negative integer. The function $L_{n+|M|}^{|M|}(\eta)$ is the associated Laguerre polynomial,

$$\eta=(eH/2\hbar c)\rho^2, \tag{35}$$

$$N_{nMk_z}^{-2}=\frac{[(|M|+n)!]^3}{n!}l_z\frac{2\hbar c}{eH}. \tag{36}$$

[36] W. Kohn, in *Solid State Physics*, edited by F. Seitz and D. Turnbull (Academic Press Inc., New York, 1957), Vol. 5, p. 284.
[37] R. B. Dingle, Proc. Roy. Soc. (London) 211, 500 (1952); M. H. Johnson and B. A. Lippmann, Phys. Rev. 76, 828 (1949).

The energy levels corresponding to these are given by[37]

$$E_{nMk_z}=\tfrac{1}{2}(\hbar\omega_c)(2n+M+|M|+1)+\hbar^2k_z^2/2\mu, \quad (37)$$

where

$$\hbar\omega_c=e\hbar H/\mu c=2(m/\mu)\beta H, \quad (38)$$

where β is the Bohr magneton. For light polarized parallel to and traveling normal to H,

$$\langle n'M'k_z'|p_z|nMk_z\rangle =\delta(k_z-k_z')\delta(M-M')\delta(n-n')\hbar k_z, \quad (39)$$

so that only virtual transitions occur, which cannot result in the real absorption of energy except in second-order processes.

For light polarized $\mathbf{E}\perp\mathbf{H}$ and for circularly polarized light traveling parallel to the field

$$\langle n'M'k_z'|p_y\pm ip_x|nMk_z\rangle$$
$$=\delta(k_z-k_z')\delta(M-M'+1)\delta(n-n')[|M|+n+1]^{1/2}$$
$$\times\frac{2}{l_z}\left(\frac{e\hbar H}{2c}\right)^{1/2}+\delta(k_z-k_z')\delta(M-M'-1)\delta(n-n')$$
$$\times[|M|+n]^{1/2}\frac{2}{l_z}\left(\frac{e\hbar H}{2c}\right)^{1/2}, \quad (40)$$

if $M>0$; and

$$\langle n'M'k_z'|p_y\pm ip_x|nMk_z\rangle$$
$$=\delta(k_z-k_z')\delta(M-M'+1)\delta(n-n'+1)[n+1]^{1/2}$$
$$\times\frac{2}{l_z}\left(\frac{e\hbar H}{2c}\right)^{1/2}+\delta(k_z-k_z')\delta(M-M'-1)\delta(n-n'-1)$$
$$\times[n]^{1/2}\frac{2}{l_z}\left(\frac{e\hbar H}{2c}\right)^{1/2},$$

if $M<0$.

Each of these correspond to the absorption or emission of a photon of energy $\hbar\omega_c$.

For a simple band the absorption spectrum for constant magnetic field consists of a single absorption line. Consideration of electron spin adds nothing new to the problem for a simple band. The momentum operator cannot flip the spin of the electron, and the cyclotron energy is independent of spin. Additional absorption peaks occur if some perturbation gives a nonuniform shift to the energy levels (as we have seen in the case of impurities and nonparabolic bands), or if some perturbation mixes states of different Landau quantum numbers.

Electron scattering can lead to states of mixed Landau levels. Consider the case of phonons. In the presence of electron-phonon interaction the no-phonon state $|nMk_z\rangle$ becomes coupled to the lattice and is given to first order in perturbation theory[38] by

$$|nMk_z\rangle|0\rangle+\sum_{\mathbf{q},n'',M'',k_z''}\frac{|n''M''k_z''\rangle b_{\mathbf{q}}^{\dagger}|0\rangle\langle 0|b_{\mathbf{q}}\langle n''M''k_z''|H_s|nMk_z\rangle|0\rangle}{E_{nMk_z}-E_{n''M''k_z''}-\hbar\omega_{\mathbf{q}}}, \quad (41)$$

where $b_{\mathbf{q}}^{\dagger}|0\rangle$ creates a phonon of wave vector $\mathbf{q}$ and energy $\hbar\omega_{\mathbf{q}}$. H_s is the perturbation term in the Hamiltonian giving the electron-phonon interaction.

The form taken by H_s depends upon the type of scattering present. We consider here only the case of LO phonons and assume an LO phonon energy ($\hbar\omega_0$) independent of $\mathbf{q}$. In this case

$$H_s=\hbar\omega_0\left(\frac{4\pi\alpha}{V/r_0^3}\right)^{1/2}\sum_{\mathbf{q}}\frac{1}{r_0q}(e^{-i\mathbf{q}\cdot\mathbf{r}}b_{\mathbf{q}}^{\dagger}+e^{i\mathbf{q}\cdot\mathbf{r}}b_{\mathbf{q}}), \quad (42)$$

where α is the electron–LO-phonon coupling constant

$$\alpha=\frac{e^2}{\hbar}\left(\frac{1}{\kappa_\infty}-\frac{1}{\kappa}\right)\left(\frac{\mu}{2\hbar\omega_0}\right)^{1/2} \quad (43)$$

and r_0 is the polaron radius

$$r_0=\left(\frac{\hbar^2}{2\mu}\Big/\hbar\omega_0\right)^{1/2}. \quad (44)$$

The matrix elements using electronic wave functions of the form of (6) are proportional to

$$\langle n''M''k_z''|e^{i\mathbf{q}\cdot\mathbf{r}}|nMk_z\rangle =\delta(k_z-k_z''+q_z)N_{n''M''k_z'}N_{nMk_z}\pi e^{i(M-M')(\pi/2+\phi_0)}I, \quad (45)$$

where $\phi_0=\tan^{-1}(q_y/q_x)$ and the integral I is given by

$$I=\int_0^\infty J_{M'-M}\left[q\left(\frac{eH}{2\hbar c}\right)^{1/2}\eta\right]e^{-\eta}\eta^{\frac{1}{2}(|M|+|M'|)} \times L^{|M|}{}_{n+|M|}(\eta)L^{|M'|}{}_{n'+|M'|}(\eta)d\eta, \quad (46)$$

where $J_{M'-M}[q(eH/2\hbar c^q)^{1/2}\eta]$ is a Bessel function.

The integral can be evaluated in several ways,[39] and one obtains a polynomial in $q_\rho^2eH/2\hbar c$. The interaction involving an LO phonon of wave vector q mixes electron states with $k_z-k_z'=q_z$ and arbitrary quantum numbers n, n', and M,M'.

[38] E. J. Johnson, *Semiconductors and Semimetals*, edited by R. K. Willardson and A. C. Beer (Academic Press Inc., New York, 1967), Vol. 3, p. 183.

[39] For example, if $|M'-M|=|M'|+|M|$ then $|I|=2^{-|M|-|M'|}\times y^{|M|+|M'|}e^{-y^2/4}L_\alpha^\beta(\frac{1}{4}y^2)L_{\alpha'}^{\beta'}(\frac{1}{4}y^2)$ with $y^2=q^2eH/2\hbar c$, $\alpha=n+|M|$, $\alpha'=n'+|M'|$, $\beta=2|M|-|M'|+n-n'$, $\beta'=2|M'|-|M|$ $n'-n$. See I. S. Gradshteyn and I. M. Ryzhik, *Tables of Integrals, Series and Products* (Academic Press Inc., New York, 1965), p. 848.

Equation (41) describes a state of mixed Landau levels. However, if one determines the momentum matrix element between states of the form of (41), one obtains simply $\langle n'M'k_z'|\mathbf{p}|nMk_z\rangle$+second-order terms. New transitions occur only in second order (two-phonon process).

If one considers a state containing a single phonon of wave vector $\mathbf{a}'$, in place of (41) one obtains

$$|n'M'k_z'\rangle b_{\mathbf{q}'}{}^{\dagger}|0\rangle+\sum_{\mathbf{q}',n'',M'',k_z''}\frac{|n''M''k_z''\rangle|0\rangle\langle 0|\langle n''M''k_z''|H_s|n'M'k_z'\rangle b_{\mathbf{q}'}{}^{\dagger}|0\rangle}{E_{n'M'k_z'}-E_{n''M''k_z''}+\hbar\omega_0}$$
$$+\sum_{\mathbf{q},n'',M'',k_z''}\frac{|n''M''k_z''\rangle b_{\mathbf{q}}{}^{\dagger}b_{\mathbf{q}'}{}^{\dagger}|0\rangle\langle 0|b_{\mathbf{q}}b_{\mathbf{q}'}\langle n''M''k_z''|H_s|n'M'k_z'\rangle b_{\mathbf{q}'}{}^{\dagger}|0\rangle}{E_{n'M'k_z'}-E_{n''M''k_z''}-\hbar\omega_0}. \quad (47)$$

With (45) as an excited state one obtains for the momentum matrix element to first order

$$\sum_{n'',M'',k_z''}\frac{\langle n'M'k_z'|\mathbf{p}|n''M''k_z''\rangle\langle 0|b_{\mathbf{q}}n''M''k_z''|H_s|nMk_z\rangle|0\rangle}{E_{nMk_z}-E_{n''M''k_z''}-\hbar\omega_0}$$
$$+\sum_{n'',M'',k_z''}\frac{\langle 0|b_{\mathbf{q}}\langle n'M'k_z'|H_s|n''M''k_z''\rangle|0\rangle\langle n''M''k_z''|\mathbf{p}|nMk_z\rangle}{E_{n'M'k_z'}-E_{n''M''k_z''}+\hbar\omega_0}. \quad (48)$$

These transitions result in the simultaneous excitation of an electron and the creation of an optical phonon. They can be considered as passing through intermediate states in which only the electron (or only the phonon) is excited.

The transitions are illustrated in Fig. 14. The scattering part of the excitation is independent of light polarization. The optical excitation is subject to the selection rules (39) and (40). The nature of the intermediate states and the energy dependence of the transition probability depend upon polarization. For $\mathbf{E}\perp\mathbf{H}$ the intermediate state lies in a Landau level adjacent to either the ground state or the excited state. For $\mathbf{E}\|\mathbf{H}$ the intermediate state is identical (neglecting the small but nonzero magnitude of the light wave vector) to either the ground state or the excited state. The density of states has a singularity as $h\nu\rightarrow\hbar\omega_0+(n+\frac{1}{2})\hbar\omega_0$ so that we might expect resonancelike behavior in the optical absorption. However, for $\mathbf{E}\|\mathbf{H}$ the optical matrix element according to (39) goes to zero with $\hbar k_z$, so that resonance behavior can be expected only for $\mathbf{E}\perp\mathbf{H}$.

Consider the effect of the finite size of the light wave vector on the cyclotron-resonance transitions. The perturbation due to light of wave vector $\mathbf{q}$ and polarization vector $\mathbf{a}$ is given by

$$e^{i\mathbf{q}\cdot\mathbf{r}}\mathbf{a}\cdot\mathbf{p}, \quad (49)$$

whereas in electric dipole transitions we set $e^{i\mathbf{q}\cdot\mathbf{r}}=1$. For $\mathbf{q}\|\mathbf{H}$ (49) becomes

$$e^{iqz}(p_y\pm ip_x). \quad (50)$$

Only the integration on z is affected leading to the selection rule $k_z'-k_z=q$. Still only one transition is allowed.

For $\mathbf{q}\perp\mathbf{H}$ and $\mathbf{a}\|\mathbf{H}$, (49) becomes

$$e^{iqx}p_z=e^{iq\rho\cos\phi}p_z. \quad (51)$$

The integration over z is unaffected, but the integration over ϕ and ρ is mathematically equivalent to (45) and transitions between nonadjacent Landau levels should occur. The transition probability would be proportional to $\hbar k_z$ and resonantlike behavior cannot be expected.

For $\mathbf{q}\perp\mathbf{H}$ and $\mathbf{a}\perp\mathbf{H}$, we have

$$e^{iqx}p_y=\sum_{n=0}^{\infty}\frac{(iqx)^n}{n!}p_y. \quad (52)$$

The integration is more complicated than in (51) but the factor e^{iqx} can be expected to induce additional transitions. The correction to the dipole approximation would be of order $(qa_c)^2$ where a_c is the cyclotron radius $\approx 10^{-6}$ cm at 25 kG. In the range of our experiments $(qa_c)^2\approx 4\times 10^{-8}$. This is to be compared to the observed factor of 10^{-2} between the harmonic and fundamental cyclotron-resonance transitions.

In the Kane theory for InSb [19] in zero order the conduction band is taken to have s-like symmetry and the valence band to have p-like symmetry. In the presence of $\boldsymbol{k}\cdot\boldsymbol{p}$ and spin-orbit interactions these bands become mixed and display nonparabolic behavior. In a magnetic field, this situation can be expected to give states of mixed Landau levels and lead to harmonics of cyclotron resonance. Bell and Rogers[40] have considered this situation and, indeed, do predict the occurrence of cyclotron-resonance harmonics in InSb. However, they predict only even harmonics with $\mathbf{E}\|\mathbf{H}$ and only odd harmonics with $\mathbf{E}\perp\mathbf{H}$.

Spin-orbit interaction results in states of mixed spin. Rashba and Sheka[41,42] have shown theoretically

[40] R. L. Bell and K. T. Rogers, Phys. Rev. **152**, 746 (1966).

[41] E. I. Rashba and V. I. Sheka, Fiz. Tverd. Tela **3**, 1735 (1960); **3**, 1863 (1960) [English transls.: Soviet Phys.—Solid State **3**, 1257 (1961); **3**, 1357 (1961)].

[42] V. I. Sheka, Fiz. Tverd. Tela **6**, 3099 (1964) [English transl.: Soviet Phys.—Solid State **6**, 2470 (1965)].

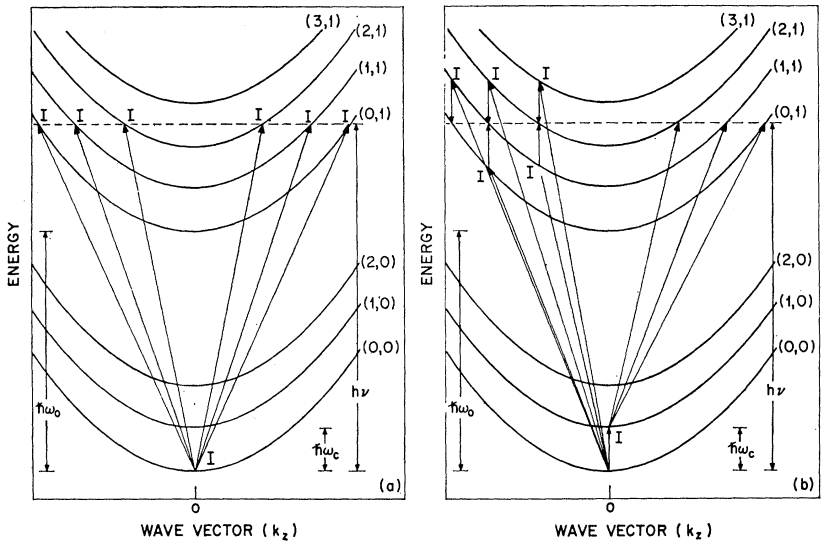

FIG. 14. Schematic energy diagram showing phonon-assisted cyclotron-resonance transitions ($M<0$) for cyclotron energy $\hbar\omega_c$, LO phonon energy $\hbar\omega_0$, and phonon energy $h\nu$. The electron is assumed to be at the bottom of the $n=0$ level in the ground state. Various intermediate states I are illustrated (a) $\mathbf{E}\|\mathbf{H}$, (b) $\mathbf{E}\perp\mathbf{H}$. For $\mathbf{E}\|\mathbf{H}$ the intermediate state is identical (within a photon wave vector) to either the ground state or the final state. There are additional intermediate states for $\mathbf{E}\perp\mathbf{H}$ identical in energy to those for $\mathbf{E}\|\mathbf{H}$.

that, as a result of this situation, transitions involving spin flip can occur (combinational resonance). Such transitions are also predicted by the work of Bell and Rogers.[40]

X. CONCLUSIONS

The conduction-band energy levels, as deduced from experiments for magnetic fields up to 27 kG involving cyclotron-resonance, combination-resonance, and the spin-resonance results of Isaacson for relatively pure samples agree to within 1% with the calculations of the energy levels using a band-edge effective mass of 0.0139, a band-edge g factor of -51.3 and a cubic equation which includes the nonparabolic effects resulting from the interaction of the conduction band with the three valence bands. The values of effective mass and g factor differ by $\sim 10\%$ from those required by the well-known Roth relation, indicating that interactions with the three valence bands alone are not sufficient to account for the experimental values. A detailed theoretical treatment of the remote band effects may serve to clarify this situation.

For magnetic fields where the cyclotron energy is comparable to an LO phonon, deviations between experiment and theory occur unless polaron self-energy effects are taken into account, as described in a previous paper.[3]

The variation of spin-resonance g factor with carrier concentration, observed by Isaacson,[7] can be quantitatively explained using the energy levels and density of states calculated. Transitions observed at higher energies and identified as phonon-assisted cyclotron resonance are found to agree with the calculations and yield a value of 24.4 meV for the LO phonon energy. Additional transitions at higher energies, identified as harmonics of cyclotron resonance, are found to agree to within 5% with the calculated energy levels and extend the range of good agreement between experiment and theory to conduction-band energies above the LO phonon energy. At higher energies yet the experimental results of Palik and Wallis appear to indicate that the agreement between experiment and theory becomes poor, but more detailed examination of the higher-energy region is needed.

Several types of transitions between magnetic energy levels have been observed which are forbidden in the simple theory. Combined resonance (which includes a spin flip) had been predicted by Rashba and Sheka.[41] Phonon-assisted cyclotron resonance is easily explained on the basis of the mixing of the combined electron-phonon states by the electron-phonon interaction. Such mixing could explain the existence of cyclotron-resonance harmonics, but predicts absorption strengths much less than those for phonon-assisted transitions, contrary to experiment. The nonzero size of the light vector could induce harmonic transitions. However, such absorption should be 10^{-8} times the fundamental CR absorption which is much less than the observed factor of 10^{-2}. Azbel'-Kaner cyclotron resonance would appear to be ruled out owing to the large skin depth in pure InSb, but could bear further consideration.

It is possible that the source of the cyclotron-resonance harmonics lies in the mixing of different Landau levels through the $\mathbf{k}\cdot\mathbf{p}$ interaction with other bands. This is a difficult theoretical problem and demands further work. The work of Bell and Rogers[40] does predict cyclotron-resonance harmonics, by this mechanism, but only odd or only even harmonics in a given polarization, which is contrary to experiment.

It is surprising that no well-defined anomalous behavior was observed in the neighborhoods where the energies of a phonon-assisted transition and a cyclotron-resonance harmonic transition tended to coincide. These would correspond to near degeneracies of one-phonon

and no-phonon levels, and one would generally expect an enhancement of the polaron self-energy. A more detailed study of these neighborhoods may yet reveal such effects.

In this work, we have ignored the possibility of an anisotropy in the conduction-band levels except to take the precaution to always orient the samples with **H** along ⟨110⟩. The main effect is expected to be in the g factor. The theoretical results[43] and the experimental results of McCombe[44] indicate that the anisotropy of the conduction-band g factor for the two lowest Landau levels is less than 4% for $H<40$ kG. For the lowest Landau level, the anisotropy is less than 2%. The anisotropy alone cannot account for a 10% remote-band contribution to the g factor.

An interesting subject for further work is to attempt to reconcile the results of this work (*intraband* transitions) with the work on the *interband* magnetoabsorption spectrum of InSb. Pidgeon-Brown type of analysis of *interband* absorption gives a conduction-band mass that lies outside of the experimental uncertainty of the *intraband* value. A detailed reexamination of the analysis of each of the experiments is needed. However, the discrepancy appears to be real and seems to indicate that there is something fundamentally different between the energy levels involved in the *intraband* experiments and those involved in the *interband* experiments in addition to effects due to excitons. A similar discrepancy appears to exist in the case of gray tin.[45]

[43] N. R. Ogg, Proc. Phys. Soc. (London) **89**, 431 (1966).
[44] B. D. McCombe, Solid State Commun. **6**, 553 (1968).

ACKNOWLEDGMENTS

It is with appreciation that we acknowledge the excellent assistance of M. J. Fulton and P. L. Ligor in carrying out the experimental work. Without their exceptional effort in preparing the samples and their meticulousness in achieving maximum performance from each part of the spectrometer system, most of the data could not have been obtained. We also acknowledge crucial discussions concerning the interpretation with L. M. Roth, H. J. Zeiger and D. M. Larsen.

[45] S. H. Groves (private communication).

PHYSICAL REVIEW B VOLUME 1, NUMBER 6 15 MARCH 1970

Calculation of the Optical Constants of PbTe from Augmented-Plane-Wave k·p Energy Bands*

DENNIS D. BUSS† AND NELSON J. PARADA‡
Department of Electrical Engineering and Center for Materials Science and Engineering, Massachusetts Institute of Technology, Cambridge, Massachusetts 02139
(Received 29 May 1969; revised manuscript received 1 August 1969)

The augmented-plane-wave method has been used to calculate the energies and wave functions of eleven levels at the origin of the Brillouin zone (BZ) of PbTe. From the wave functions, momentum matrix elements have been calculated and these have been used in a **k·p** expansion of the energy bands. The **k·p** secular equation has been solved throughout the BZ and the results have been used to calculate the interband contribution to the optical constants in the random-phase approximation. The calculated value of $\epsilon_1(\omega=0)$ (40.0) compares favorably to the measured value ($\epsilon_\infty=31.8$), and the calculated reflectivity agrees with experiment to within 10% in the frequency range $0<\hbar\omega<3$ eV.

I. INTRODUCTION

In order to make a calculation of the optical dielectric constant $\epsilon(\omega)=\epsilon_1(\omega)+i\epsilon_2(\omega)$ of a material, it is necessary to know the resonant frequency and the oscillator strength of every transition in the material, that is, it is necessary to know the energy differences between the occupied and the unoccupied bands everywhere in **k** space, and the momentum matrix elements coupling these bands. Therefore, by comparing these calculations with measured optical properties, it is possible to test the validity of the wave functions from which momentum matrix elements are calculated as well as the accuracy of the energy bands.

First-principles calculations are capable of yielding the information required to calculate optical constants. For example, Herman *et al.* have used a combination of the orthogonalized-plane-wave (OPW) method and the pseudopotential method to obtain the optical spectrum of many materials including the Pb salts.[1] OPW energy bands are calculated at a few high-symmetry points and pseudopotential band parameters are adjusted to fit the OPW results. Optical properties are then obtained from the pseudopotential bands either by as-

* Work supported in part by the National Science Foundation and in part by the U. S. Army Research Office (Durham).
† Present address: Central Research Laboratory, Texas Instruments Inc., Dallas, Tex.
‡ Present address: Departamento de Fisica, Universidade de Sao Paulo, Sao Paulo, Brazil.

[1] F. Herman, R. L. Kortum, I. B. Ortenburger, and J. P. Van Dyke, J. Phys. (Paris), Suppl. **29**, 62 (1968), and references cited here.